

Macroscopic theory of heavy-ion fusion reactions

S.-W. Hong

Institut für Kernphysik, Kernforschungsanlage Jülich, D-5170 Jülich, West Germany

Y. J. Lee and B. T. Kim

Department of Physics, Sung Kyun Kwan University, Suwon 440-746, South Korea

D. Cha

Department of Physics, Inha University, Incheon 402-751, South Korea

(Received 31 October 1988)

We have studied the heavy-ion fusion reactions by a macroscopic model which was proposed by Bertsch several years ago. It employed the Newtonian dynamics and was constructed in such a way that the essential features of time-dependent Hartree-Fock results could be reproduced. We have applied the model to fusion of light heavy-ion systems leading to the same compound nucleus ^{56}Ni . It is shown that the model, being incorporated with the angular-momentum-dependent extra-push energy of Swiatecki, can account well for the fusion cross sections up to very high energies where cross section decreases as energy increases, and that the main reason for the decrease is the opening of the low angular momentum window.

The excitation functions of heavy-ion fusion reactions at the incident center-of-mass energies ($E_{\text{c.m.}}$) higher than the Coulomb barrier show an interesting shape. As $E_{\text{c.m.}}$ increases, the fusion cross section monotonically increases until the energy becomes about twice the Coulomb barrier height (region I), and then suddenly the fusion cross section becomes more or less constant (region II). There are some experimental data^{1,2} indicating another energy region where the fusion cross section decreases as $E_{\text{c.m.}}$ gets even higher (region III). The fusion cross section in region I, where it exhausts most of the total reaction cross section, is fairly well understood, but it still remains unclear what determines the characteristic shape of the fusion cross section in regions II and III, al-

though there has been done a number of theoretical studies in these energy regions.^{1,3-5} It has been a while since time-dependent Hartree-Fock (TDHF) theory was applied to fusion reaction and predicted the low-angular-momentum (l) window at the energies in regions II and III.⁶ Experimental examinations were made at the energies in region II, but a firm conclusion on the existence of a low- l window could not be reached.⁷

Several years ago, Bertsch proposed a macroscopic model for heavy-ion collisions.⁸ It employed the Newtonian dynamics for the relative coordinate of the centers of mass of two colliding nuclei (the only one variable necessary in the model), and it was constructed in such a way that practically all the essential features of TDHF results could be reproduced. The macroscopic forces used in the equations of motion were expressed in terms of the neck radius, which in turn evolves in a similar way as that of TDHF calculations. The model, which

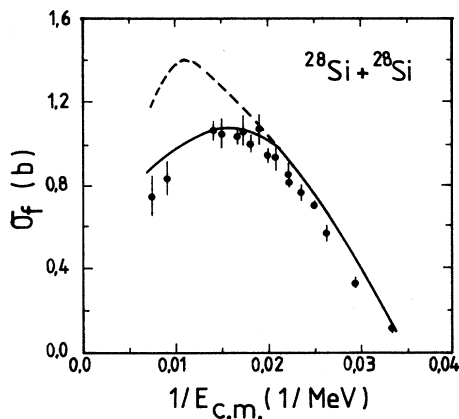


FIG. 1. The fusion excitation function of the $^{28}\text{Si} + ^{28}\text{Si}$ system. The fusion cross section is calculated by the neck model (dashed curve) and by the neck model incorporated with the angular-momentum-dependent extra-push energy (solid curve).

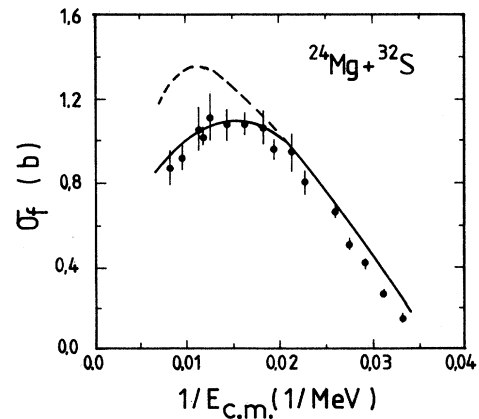


FIG. 2. Same as Fig. 1 but for the $^{24}\text{Mg} + ^{32}\text{S}$ system.

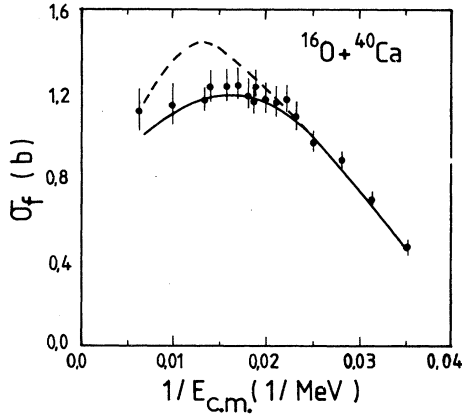


FIG. 3. Same as Fig. 1 but for the $^{16}\text{O} + ^{40}\text{Ca}$ system.

we will call the “neck” model hereafter, was tested later by Bonasera, Bertsch, and El-Sayed against the results of TDHF theory.⁹ Their results have also shown the low- l window of fusion for light heavy-ion systems such as $^{20}\text{Ne} + ^{20}\text{Ne}$ and $^{28}\text{Si} + ^{28}\text{Si}$. However, the data at higher energies were not available at the time, and no decisive conclusion on the existence of the low- l window could be drawn. In this work, we want to analyze the recent fusion data, especially in regions II and III, by means of the neck model.

We consider the fusion reactions of $^{28}\text{Si} + ^{28}\text{Si}$, $^{32}\text{S} + ^{24}\text{Mg}$, and $^{16}\text{O} + ^{40}\text{Ca}$, which lead to the same compound nucleus ^{56}Ni . In Figs. 1, 2, and 3, the recent experimental data for $^{28}\text{Si} + ^{28}\text{Si}$, $^{32}\text{S} + ^{24}\text{Mg}$, and $^{16}\text{O} + ^{40}\text{Ca}$ obtained by Rosner *et al.*,¹⁰ Hinnefeld *et al.*,² and Vigdor *et al.*,¹¹ respectively, are plotted together with the already existing data taken by others.¹²

The results of the neck model calculations are shown in Figs. 1, 2, and 3 by the dashed curves. The calculations were done in the same way as described in Ref. 8. The neck model calculations agree quite well with the data in region I. In addition, the characteristic shape of the fusion cross section in regions II and III is also reproduced, although the calculated cross sections overestimate the data.

The results obtained by the neck model can be understood more clearly in the fusion contour diagram where $E_{c.m.}$ is plotted versus the impact parameter. The dashed curves in Fig. 4 are the fusion contour obtained from the neck model for the $^{28}\text{Si} + ^{28}\text{Si}$ system, and it is the same as Fig. 7 of Ref. 8, since we have used the same model parameters. The sharp cutoff model lets us calculate the fusion cross section at each energy as

$$\sigma_f = \pi(b_{\max}^2 - b_{\min}^2), \quad (1)$$

where b_{\max} and b_{\min} are, respectively, the maximum and

$$E_x(l) = \begin{cases} 0 & \text{for } (Z^2/A)_{\text{eff}}(l) < (Z^2/A)_{\text{eff}}^{\text{thr}} \\ a_0^2 \eta_0 [(Z^2/A)_{\text{eff}}(l) - (Z^2/A)_{\text{eff}}^{\text{thr}}]^2 & \text{for } (Z^2/A)_{\text{eff}}(l) > (Z^2/A)_{\text{eff}}^{\text{thr}} \end{cases}, \quad (3)$$

where

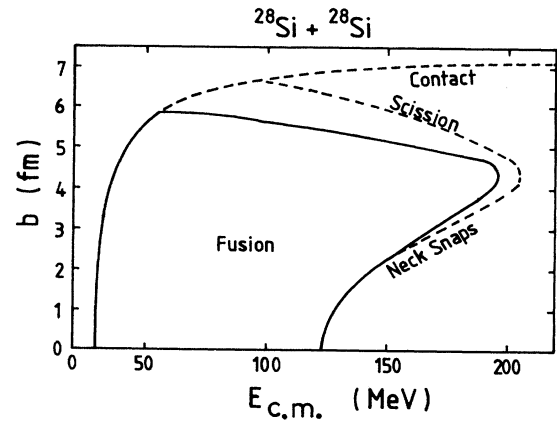


FIG. 4. The fusion contour diagram for the $^{28}\text{Si} + ^{28}\text{Si}$ system. The contour is calculated by the neck model (dashed curve) and by the neck model incorporated with the angular-momentum-dependent extra-push energy (solid curve).

minimum impact parameters where the fusion takes place. The neck model prediction of the fusion cross section in region I in Fig. 1 is determined by the contact line in Fig. 4, which corresponds to the maximum impact parameter with which the approaching nuclei touch each other. This continues until the scission starts, and then region II begins, resulting in the saturation of the fusion cross section. Along the scission line, the nuclear force just balances the centrifugal and Coulomb repulsion, and the neck barely holds the nuclei from being separated. The sudden decrease in the fusion cross section when region III starts is caused by the neck snapping which opens the low- l window in the fusion contour diagram. In this region, the extremely large tensile strength of nuclear matter results in sudden breakage of the neck.

The neck model predictions of the fusion cross section, however, deviate from the data significantly as the energy becomes larger in all the three cases of Figs. 1, 2, and 3. The calculated region II occurs at much higher energy than the experimental one, and the calculated cross sections overestimate the measured ones by a large amount.

The overestimation of the fusion cross section at high energies is a common feature in various theoretical models.³ Such a problem was successfully accounted for by an extra-push energy which Swiatecki recently introduced into his potential model of colliding heavy ions.¹³ The extra-push energy is expressed in terms of the effective asymmetry parameter $(Z^2/A)_{\text{eff}}$ defined in Ref. 13 as

$$(Z^2/A)_{\text{eff}} = 4Z_1 Z_2 / [A_1^{1/3} A_2^{1/3} (A_1^{1/3} + A_2^{1/3})]. \quad (2)$$

Here Z 's and A 's refer to the atomic number and mass number of the colliding nuclei, respectively. Then the extra-push energy which is dependent on the angular momentum transfer l , $E_x(l)$, is given by

$$\eta_0 = 7.6 \times 10^{-4} A_1^{1/3} A_2^{1/3} (A_1^{1/3} + A_2^{1/3})^2 / (A_1 + A_2) \quad (4)$$

and

$$(Z^2/A)_{\text{eff}}(l) = (Z^2/A)_{\text{eff}} + 95.86 f^2 l^2 (A_1 + A_2) / [A_1^{4/3} A_2^{4/3} (A_1^{1/3} + A_2^{1/3})^2] . \quad (5)$$

In this study, we want to incorporate the effect of the angular-momentum-dependent extra-push energy with the neck model. It is done by taking $E_{\text{c.m.}} + E_x(l)$ instead of $E_{\text{c.m.}}$ in our neck model calculations, and by treating it as an effective center-of-mass energy. In our calculations, a_0 and $(Z^2/A)_{\text{eff}}^{\text{thr}}$ in Eq. (3) are adjusted for each system, and the adopted values are listed in Table I. The quantity f in Eq. (5) represents the final angular momentum fraction. It is also taken as a parameter in the present calculation, and the adopted values are also listed in Table I.

The results of new calculations are shown by the solid curves in Figs. 1, 2, and 3. They fit very nicely the data points throughout regions I, II, and III except at the two highest energies of the most asymmetric system of $^{16}\text{O} + ^{40}\text{Ca}$. However, for these data points there is an experimental indication showing a possibility of the contribution from incomplete fusion to the fusion cross section.¹⁴ After including the extra-push energy, only the scission line, the solid line in Fig. 4, is changed appreciably and all other lines remain more or less the same, and we still have the low- l window intact. We can see from the new contour that the upper boundary of the fusion cross sections is reduced. This reduction of the contribution to fusion from the high- l components comes from the extra push. Incidentally, Swiatecki's extra-push energy,¹³ which is necessary even at the zero impact parameter for the systems with a large asymmetric parameter $(Z^2/A)_{\text{eff}}$, was taken care of adequately by the original neck model, as can be seen from Fig. 8 of Ref. 8.

Another reason that the fusion cross sections in region III are well reproduced is that the low- l window is opened at high energies. It contrasts quite sharply with most other models that fit the data in region III, in that they limit only the higher components of the angular momentum or the maximum impact parameter. However, our good fit to the data alone may not be taken as concrete evidence for the existence of the low- l window, considering the number of parameters used in the extra-push energy, even though the adopted parameters are reasonable compared to other studies.

TABLE I. Parameters adopted in the calculations in evaluating the extra-push energy given by Eq. (3) of the text.

System	$^{28}\text{Si} + ^{28}\text{Si}$	$^{32}\text{S} + ^{24}\text{Mg}$	$^{16}\text{O} + ^{40}\text{Ca}$
a_0	6.7	6.2	5.3
f	0.714	0.714	0.650
$(Z^2/A)_{\text{eff}}^{\text{thr}}$	24.00	23.50	21.00

In the sharp cutoff approximation from which Eq. (1) follows, each partial wave less than L_{max} and larger than L_{min} contributes to the fusion cross section by

$$\sigma_l = \pi \hbar^2 (2l + 1) / 2\mu E_{\text{c.m.}} , \quad (6)$$

where μ is the reduced mass of the system. Then the average of l , which has participated in the fusion, becomes

$$\langle l \rangle = 2L_{\text{max}} [1 + (L_{\text{min}}/L_{\text{max}})^2 / (1 + L_{\text{min}}/L_{\text{max}})] / 3 . \quad (7)$$

The second term in the right-hand side of Eq. (7) shows how much $\langle l \rangle$ deviates from the case when there is no low- l cut. The deviation becomes about 17% when $L_{\text{min}}/L_{\text{max}} = 0.5$, and about 30% when $L_{\text{min}}/L_{\text{max}} = 0.7$, which corresponds to $E_{\text{c.m.}} = 180$ MeV in our $^{28}\text{Si} + ^{28}\text{Si}$ fusion contour diagram. Therefore, it might be possible to test the existence of the low- l window by measuring the spin distributions of the fused system at high energies in region III.

In summary, we have applied the neck model, which is a macroscopic model that mimics the dynamics of the TDHF theory, to fusion reaction of light heavy-ion systems leading to the same compound nucleus ^{56}Ni . The neck model is incorporated with the l -dependent extra-push energy, and it is demonstrated that the neck model can account for the fusion cross section very successfully up to very high energies in region III. The main reason that the decrease in the fusion cross section with increasing $E_{\text{c.m.}}$ is well reproduced in region III is the opening of the low- l window which was also predicted by TDHF calculations. And the results may be counterchecked by measuring, for instance, the spin distributions of the fused systems at the energies in region III. Through the present study, it seems to us that the neck model can not only be applied to a variety of interesting phenomena of the heavy-ion systems where the TDHF calculations are not feasible due to computational difficulties, but also can provide macroscopic concepts for future development of microscopic theories.

We are very grateful to Professor G. F. Bertsch for his correspondence and valuable comments. This work was supported in part by the Ministry of Education, Korea, through the Basic Science Institute Program, 1988.

- ¹Y. Nagashima *et al.*, Phys. Rev. C **33**, 176 (1986).
²J. D. Hinnefeld *et al.*, Phys. Rev. C **36**, 989 (1987).
³J. R. Birkelund and J. R. Huizenga, Annu. Rev. Nucl. Part. Sci. **33**, 265 (1983).
⁴S.-W. Hong, Ph.D. thesis, University of Texas at Austin, 1987.
⁵B. T. Kim and D. Cha, Phys. Rev. C **35**, 1605 (1987).
⁶P. Bonche, B. Grammaticos, and S. Koonin, Phys. Rev. C **17**, 1700 (1978).
⁷B. Fernandez *et al.*, Nucl. Phys. **A306**, 259 (1978).
⁸G. F. Bertsch, Michigan State University Report (1982).
⁹A. Bonasera, G. F. Bertsch, and E. N. El-Sayed, Phys. Lett. **141B**, 9 (1984).
¹⁰G. Rosner *et al.*, Argonne National Laboratory Annual Report ANL-83-25, 1983.
¹¹S. E. Vigdor *et al.*, Phys. Rev. C **20**, 2147 (1979).
¹²See references quoted in Ref. 2.
¹³W. J. Swiatecki, Phys. Scr. **24**, 113 (1981).
¹⁴Y. Chan *et al.*, Phys. Rev. C **27**, 447 (1983).